Advances in Computational Design, *Vol. 2, No. 2 (2017) 107-119*
DOI: https://doi.org/10.12989/acd.2017.2.2.107

A study on thermo-mechanical behavior of MCD through bulge test analysis

Wael A. Altabey*[1,2]

[1]*International Institute for Urban Systems Engineering, Southeast University, 210096, Nanjing, China*
[2]*Department of Mechanical Engineering, Faculty of Engineering, Alexandria University, 21544, Alexandria, Egypt*

(Received August 28, 2016, Revised November 21, 2016, Accepted January 19, 2017)

Abstract. The Micro circular diaphragm (MCD) is the mechanical actuator part used in the micro electro-mechanical sensors (MEMS) that combine electrical and mechanical components. These actuators are working under harsh mechanical and thermal conditions, so it is very important to study the mechanical and thermal behaviors of these actuators, in order to do with its function successfully. The objective of this paper is to determine the thermo-mechanical behavior of MCD by developing the traditional bulge test technique to achieve the aims of this work. The specimen is first pre-stressed to ensure that is no initial deflection before applied the loads on diaphragm and then clamped between two plates, a differential pressure (P) and temperature (T_b) is leading to a deformation of the MCD. Analytical formulation of developed bulge test technique for MCD thermo-mechanical characterization was established with taking in-to account effect of the residual strength from pre-stressed loading. These makes the plane-strain bulge test ideal for studying the mechanical and thermal behavior of diaphragm in both the elastic and plastic regimes. The differential specimen thickness due to bulge effect to describe the mechanical behavior, and the temperature effect on the MCD material properties to study the thermal behavior under deformation were discussed. A finite element model (FEM) can be extended to apply for investigating the reliability of the proposed bulge test of MCD and compare between the FEM results and another one from analytical calculus. The results show that, the good convergence between the finite element model and analytical model.

Keywords: bulge test; thermo-mechanical behavior; micro circular diaphragm; finite-element analysis; and MATLAB software

1. Introduction

The micro circular diaphragm (MCD) is the most important part in numerous engineering and bioengineering sensors applications such as the micro electro-mechanical sensors (MEMS), they range in size from the sub micrometer (μm) level to the millimeters (mm) level, e.g., the pressure sensors normally have a MCD that deforms in the presence of pressure difference. The deformation is converted in an electrical signal that appears at the sensor output. Many of the materials that are used for MCD are quite common, e.g., Bronze, Brass, Aluminum and Stainless steel.

*Corresponding author, Assistant Professor, E-mail: wael.altabey@gmail.com

http://www.techno-press.org/?journal=acd&subpage=7 ISSN: 2283-8477 (Print), 2466-0523 (Online)

The hydrostatic bulging of metal sheets, more commonly known as the bulge test, is a preferred method for the determination of the mechanical characteristics of metals. Numerous works to predict the behavior and characteristics of metals under bulging have been undertaken and reported here, the first application bulge test technique, conducted by (Hill 1950, Mellor 1956) on the bulging of circular diaphragms being the earlier contributions in this field. Chater and Neale (1983) have examined the large strain behavior of a circular membrane under uniform hydrostatic pressure for materials with transversely isotropic plastic properties. They are first applied to derive the governing equations for the pressurized membrane. (Ilahi *et al.* 1981, Ilahi and Paul 1985, Kular and The 1972) have investigated the hydrostatic bulging of anisotropic Aluminum sheets by comparing the experimental results with the theoretical predicted values. Comparison is made with theoretical and experimental results obtained also by other investigators (Brandon *et al.* 1979, Tang 1982, Hill 1990). On the other way of the bulge test research goals in this research decade to obtain the influence of material parameters on the hydrostatic bulging, Zeghloul *et al.* (1991) have examined the plastic bulging of pressurized circular membranes with particular attention to the effect of material parameters on the inherent in homogeneity of the test. Also, Wang and Shammamy (1969) were analyzed the hydrostatic bulging of a circular sheet clamped on the basis of both an incremental theory and the corresponding total strain theory of plasticity to show the effects of material types. The material of the sheet is assumed to have strain-hardening capacity and to be anisotropic in the thickness direction. They found that the incremental theory predicts that as the polar strain increases the pressure reaches a maximum and then decreases, whereas the total strain theory gives unsatisfactory results.

The objective of the theoretical and numerical work to date has been to predict the behavior and characteristics of the metal under the hydrostatic bulging process and to determine the relationships among pressure, strain, and geometrical changes as accurately as possible. Storakers (1966) was being the earlier work used the numerical solution to study the bulge test. He presented an analysis of the plastic deformation including instability phenomena of a circular membrane subject to one-sided hydrostatic pressure. Equations determining stresses and strains are given for the deformation process of materials with a parabolic stress-strain curve. Numerical solutions have been carried out for some special cases. Then several researchers used the numerical solution to save time effort in experimental work and to check validity the results that are come from experimental and theoretical works. Ahmed and Hashmi (1998) were studied the effect of combined pressure and in-plane compressive load on the sheet-plate by the finite-element method. The contact condition between the die and the sheet-plate is also taken into consideration in the analysis. Further, the analysis is undertaken also for the pressure-only loading case and the results are compared. Wan *et al.* (2003) measured a tensile residual stress in a plate or membrane clamped at the perimeter by either applying a uniform hydrostatic pressure or a central load via a cylindrical punch (with several different loading configurations). Analytical constitutive relations are derived here based on an average membrane stress approximation and are compared to finite element analysis results. Also in the last decades the numerical solution is playing important side in bulge test technique to determine of the mechanical characteristics of metals.

Since this time, the bulge test technique research was taken the way of investigating the accuracy and reliability to study the mechanical properties of thin film materials, and effects parameters on it to proof the bulge test performance and capabilities as the research work by Itozaki (1982) showed that failure to include the initial height of the membrane in the analysis leads to an apparent nonlinear elastic behavior of the film, then also Small *et al.* (1992) analyzed the influence of initial film conditions such as film wrinkling, residual stress, and initial height of

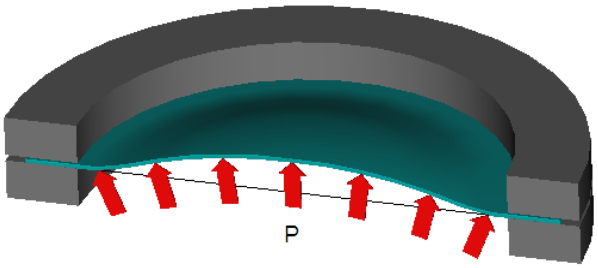

Fig. 1 Schematic representation of the bulge test

the membrane using finite element analysis. The accuracy and reliability of the bulge test has been analyzed by many investigators (Vlassak 1994, Grolleau *et al.* 2008, Jung *et al.* 2012, Jung *et al.* 2013, Yang *et al.* 2014, Zhang *et al.* 2015, Huang *et al.* 2016, Suttner and Merklein 2016). These authors point out that the, although the determination of the plane-strain modulus in the light of the plane-strain bulge equation is fairly accurate, the calculation of the residual stress is not satisfied as expected, especially for low residual stress. Finally, some of these work proposed an approach for analyzing bulge test data, which will improve the accuracy and reliability of this bulge test technique.

The plane-strain bulge test is a powerful new technique for measuring the mechanical properties of thin films. In this technique, the stress-strain curve of a thin film is determined from the pressure-deflection behavior of the circular membrane made of the film of interest, see Fig. 1. For a thin membrane in a state of plane strain, film stress and stain are distributed uniformly across the membrane width, and simple analytical formulae for stress and strain can be established (Xiang *et al.* 2005).

In this study, the developed traditional bulge test technique to determine the thermo-mechanical behavior of MCD. The specimen is first pre-stressed to ensure that is no initial deflection before applied the loads on diaphragm and then clamped between two plates, a differential pressure (P) and temperature (T_b) is leading to a deformation of the MCD. The partial deferential equation of MCD was derived according to diaphragm conditions to establish the analytical solution of bulged MCD for thermo-mechanical characterization with taking in-to account effect of the residual strength from pre-stressed loading. A finite element analysis is carried out to verify the accuracy of the proposed bulge test of MCD. The comparison between the FEM results and analytical calculus results was occurred. The results show that, the good convergence between the finite element model and analytical model which confirm the successes of the presented technique. The simulation results were obtained using MATLAB software tool boxes.

2. The bulge test of MCD model

2.1 Geometrical model

Fig. 2(a) represents the geometrical model of MCD before and after displacement at left half and right half side respectively. As shown in the figure the MCD has a radius *a* and the thickness *h*. The diaphragm is first pre-stress under radial stress σ_0 to ensure the initial deflection before applied the load equal zero and then clamped between two plates. The upper side of the plate is

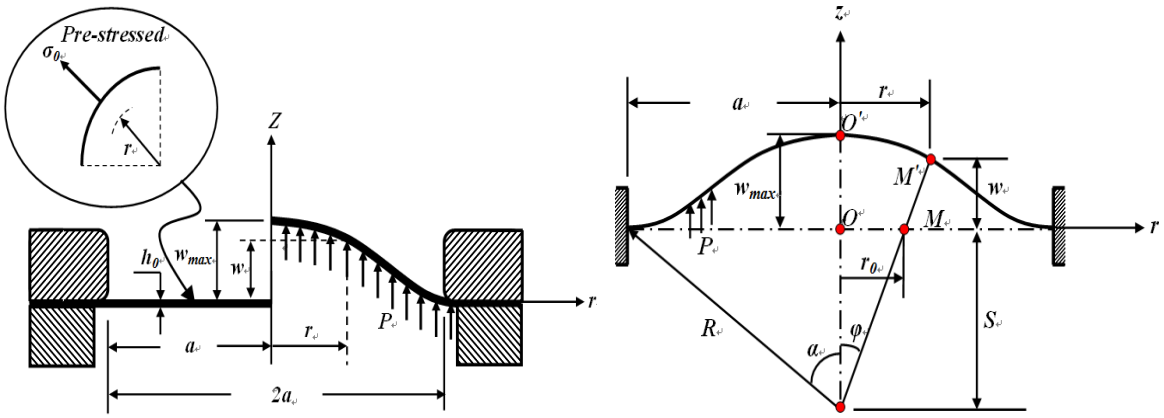

(a) The geometrical model (b) Schematic of deformation modeling

Fig. 2 The model of MCD element

exposed to room temperature T_t=25℃ and the lower side of the film is subjected to thermo-fluid media with pressure P and temperature T_b. Fig. 2(b) represents the dome profile of the diaphragm deformation.

2.2 Formulation

The equation of motion governing the MCD under the assumption of the classical deformation theory in terms of the plate deflection $W(x, y, t)$ is given by Ventsel and Krauthammer (2001) as

$$\frac{\partial^2 m_r}{\partial r^2} - \frac{2}{r}\frac{\partial^2 m_{rt}}{\partial r \partial \theta} + \frac{\partial^2 m_t}{\partial \theta^2} = -\rho h \frac{\partial^2 w}{\partial t^2} \tag{1}$$

Where w is the transverse deflection, ρ=the density per unit area of the plate and h is the MCD thickness at any point could be calculated from the geometry shape of Fig. 2(b) by equations

$$h = h_0 \left(\frac{\sin \alpha}{\alpha}\right)^2 \left(\frac{\varphi}{\sin \varphi}\right) \tag{2}$$

$$\alpha = sin^{-1}\left(\frac{a}{R}\right) \tag{3}$$

$$\varphi = tan^{-1}\left(\frac{r}{S}\right) \tag{4}$$

The radius of curvature R, see Fig. 2(b), is

$$R = \frac{a^2 + w_{max}}{2w_{max}} \tag{5}$$

$$S = \frac{a}{tan\, \alpha} \tag{6}$$

The bending and twisting moments (m_r, m_t, m_{rt}) and shear forces (q_r, q_t) in terms of displacements and thermal effect term we can be written in the following form

$$\left.\begin{aligned} m_r &= -D\left[\frac{\partial^2 w}{\partial r^2} + \upsilon\left(\frac{1}{r}\frac{\partial w}{\partial r} + \frac{1}{r^2}\frac{\partial^2 w}{\partial \theta^2}\right) + \alpha_T \frac{\Delta T}{h}(1-\upsilon)\right] \\ m_t &= -D\left[\frac{1}{r}\frac{\partial w}{\partial r} + \frac{1}{r^2}\frac{\partial^2 w}{\partial \theta^2} + \upsilon\frac{\partial^2 w}{\partial r^2} + \alpha_T \frac{\Delta T}{h}(1-\upsilon)\right] \\ m_{rt} &= m_{tr} = -D(1-\upsilon)\left(\frac{1}{r}\frac{\partial^2 w}{\partial r \partial \theta} - \frac{1}{r^2}\frac{\partial w}{\partial \theta}\right) \\ q_r &= -D\frac{\partial}{\partial r}(\nabla_r^2 w) - \frac{\partial m_T}{\partial r} \\ q_t &= -D\frac{1}{r}\frac{\partial}{\partial \theta}(\nabla_r^2 w) - \frac{\partial m_T}{\partial \theta} \end{aligned}\right\} \quad (7)$$

The stress components σ_r, σ_t and shear stresses τ_{tr} produce bending moments in the MCD element in a manner similar to that in elementary beam theory (Ventsel and Krauthammer 2001). Thus, by integration of the normal and shear stress components, the bending moments, acting on the MCD element, are obtained

$$m_r = \int_{-(h/2)}^{+(h/2)} \sigma_r z dz, m_t = \int_{-(h/2)}^{+(h/2)} \sigma_t z dz \text{ and } m_{rt} = \int_{-(h/2)}^{+(h/2)} \sigma_{rt} z dz$$

Similarly, the formulas for the plane stress components of the MCD, from Eq. (7) are written in the following form

$$\sigma_r = \frac{12 m_r}{h^3} z, \quad \sigma_t = \frac{12 m_t}{h^3} z, \quad \tau_{rt} = \tau_{tr} = \frac{12 m_{tr}}{h^3} z \quad (8)$$

The flexural rigiditie D of the plate is given by

$$D = \frac{E h^3}{12(1-\upsilon^2)} \quad (9)$$

Where E are the Young's moduli, ν is the Poisson's ratio. Thus, the governing partial differential equation of the MCD subjected to thermal and mechanical load as shown in Fig. 2(a) is reduced to

$$\nabla_r^4 w \equiv \frac{\partial^4 w}{\partial r^4} + \frac{2}{r}\frac{\partial^3 w}{\partial r^3} - \frac{1}{r^2}\frac{\partial^2 w}{\partial r^2} + \frac{1}{r^3}\frac{\partial w}{\partial r} + \frac{2}{r^2}\frac{\partial^4 w}{\partial r^2 \partial \theta^2} - \frac{2}{r^3}\frac{\partial^3 w}{\partial \theta^2 \partial r} + \frac{4}{r^4}\frac{\partial^2 w}{\partial \theta^2} + \frac{1}{r^4}\frac{\partial^4 w}{\partial \theta^4} = \frac{P+P_T}{D} \quad (10)$$

Where P_T is the thermal load applied on MCD is given by

$$P_T = \nabla_r^2 m_T \quad (11)$$

Where $\nabla_r^2 = \left(\frac{\partial^2}{\partial r^2} + \frac{1}{r}\frac{\partial}{\partial r} + \frac{1}{r^2}\frac{\partial^2}{\partial \theta^2}\right)$ and m_T is the thermal equivalent bending moment, it is obtained by equation

$$m_T = \frac{\alpha_T E}{(1-\upsilon)} \int_{-(h/2)}^{+(h/2)} \Delta T z dz = D\alpha_T \frac{T_t - T_b}{h}(1+\upsilon) \quad (12)$$

2.3 The MCD pre-stress modeling

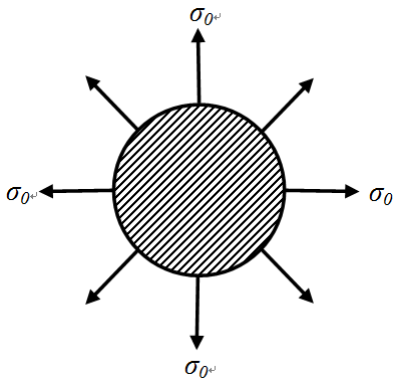

Fig. 3 The pre-stress of MCD model

Considering the pre-existence of an equi-biaxial residual stress per unit length σ_0 before applying the load on the MCD at radial direction to ensure that the deflection w_0=0 as shown on the Fig. 3, the pre-stress must be placed in the equation of the radial stress before calculating m_r.

From the previous equations for m_r and σ_r of MCD we can be written these after added the pre-stress term in the following form

$$\sigma_r = -z\left(\frac{E}{(1-\upsilon^2)}\left[\frac{\partial^2 w}{\partial r^2}+\upsilon\left(\frac{1}{r}\frac{\partial w}{\partial r}+\frac{1}{r^2}\frac{\partial^2 w}{\partial \theta^2}\right)+\alpha_T\frac{\Delta T}{h}(1-\upsilon)\right]+\frac{\sigma_0}{(1-\upsilon)}\right)$$
$$\because m_r = \int_{-(h/2)}^{+(h/2)} \sigma_r z dz \tag{13}$$

$$m_r = \int_{-(h/2)}^{+(h/2)} z\left(\frac{-E}{(1-\upsilon^2)}\left[\frac{\partial^2 w}{\partial r^2}+\upsilon\left(\frac{1}{r}\frac{\partial w}{\partial r}+\frac{1}{r^2}\frac{\partial^2 w}{\partial \theta^2}\right)+\alpha_T\frac{\Delta T}{h}(1-\upsilon)\right]+\frac{\sigma_0}{(1-\upsilon)}\right)dz \tag{14}$$

$$m_r = -D\left[\frac{\partial^2 w}{\partial r^2}+\upsilon\left(\frac{1}{r}\frac{\partial w}{\partial r}+\frac{1}{r^2}\frac{\partial^2 w}{\partial \theta^2}\right)+\alpha_T\frac{\Delta T}{h}(1-\upsilon)\right]+\frac{h^3\sigma_0}{12(1-\upsilon)} \tag{15}$$

3. Method of solution

When an applied loading and end restraints of the MCD are independent of the angle φ then the deflection of the diaphragm and the stress resultants and stress couples will depend upon the radial position r only. Such a bending of the MCD is referred to as axially symmetrical and the following simplifications can be made

$$\frac{\partial^k ()}{\partial \theta^k} = m_{rt} = q_t = 0; \quad k = 1,2,3,4 \tag{16}$$

The differential equation of the deflected surface of the circular plate, Eq. (10), reduces now to

$$\frac{d^4 w}{dr^4}+\frac{2}{r}\frac{d^3 w}{dr^3}-\frac{1}{r^2}\frac{d^2 w}{dr^2}+\frac{1}{r^3}\frac{dw}{dr}=\frac{P+P_T}{D} \tag{17}$$

Eq. (17) appears in the form

$$\frac{1}{r}\frac{d}{dr}\left\{\frac{1}{r}\frac{d}{dr}\left[\frac{1}{r}\frac{d}{dr}\left(r\frac{dw}{dr}\right)\right]\right\}=\frac{P+P_T}{D} \tag{18}$$

Where Eq. (18) the governing partial differential equation of the axisymmetric thermo-mechanical bending of MCD and w is the deflection of the diaphragm at axial direction we can be obtained by solve the partial differential Eq. (18).

Rigorous solution of Eq. (18) is obtained as the sum of the complementary solution of the homogeneous differential equation, w_h, and the particular solution, w_p, i.e.,

$$w = w_h + w_p \tag{19}$$

The complementary solution of Eq. (18) is given by

$$w_h = C_1 \ln r + C_2 r^2 \ln r + C_3 r^2 + C_4 \tag{20}$$

Where C_i(i=1,2,3,4) are constants that can be evaluated from the boundary conditions. The particular solution, w_p, is obtained by successive integration of Eq. (18)

$$w_p = \int \frac{1}{r}\int r \int \frac{1}{r}\int \frac{r(P(r)+P_T(r))}{D} drdrdrdr \tag{21}$$

The boundary conditions for MCD with clamped edge as shown in Fig. 1 are

$$\left.\begin{array}{l} w = 0\big|_{r=a} \\ \dfrac{\partial w}{\partial r} = 0\Big|_{a=0} \end{array}\right\} \tag{22}$$

For the solid plate, which contains no concentrated loads at r=0, it is easy to see that the terms involving the logarithms in Eq. (20) yield an infinite displacement and bending moment, and the shear force for all values of C_1 and C_2, except zero; therefore, C_1=C_2=0. Thus, for a solid circular plate subjected to an axisymmetric distributed load with arbitrary boundary conditions, the deflection surface is given by

$$w = C_3 r^2 + C_4 + w_p \tag{23}$$

The constants of integration C_3 and C_4 in this equation are determined from boundary conditions and we obtain

$$C_3 = -\frac{Pa^2}{32D} - \frac{m_T}{D}\left[\frac{1}{4}\ln a - \frac{1}{8}\right] \tag{24}$$

$$C_4 = \frac{Pa^4}{64D} + \frac{a^2 m_T}{8D} \tag{25}$$

And after some manipulation, the transverse deflection w, bending moments (m_r, m_t) and shear forces (q_r) will becomes

$$w = \frac{P}{64D}(a^2 - r^2)^2 + \frac{m_T}{4D} r^2(\ln r - \ln a) + \frac{m_T}{8D}(a^2 - 3r^2) \tag{26}$$

Table 1 Material thermal and mechanical properties

Material	E (Gpa)	G(Gpa)	υ	$K(W.C^{-1}.m^{-1})$	$\alpha(C^{-1})$
Al-Pure	71.7	26.9	0.333	237	23 E-6

Table 2 Loading history

Pressure P(MPa)	P_1=100	P_2=200	P_3=300	P_4=400
Temperature T_b(C°)	T_1=50	T_2=100	T_3=150	T_4=200

$$m_r = \frac{P}{16}\left(a^2(\upsilon+1) - r^2(3+\upsilon)\right) + \frac{m_T}{2}(\upsilon+1)(\ln a - \ln r) - \frac{m_T}{2} - D\alpha_T\frac{\Delta T}{h}(1-\upsilon) + \frac{h^3\sigma_0}{12(1-\upsilon)} \tag{27}$$

$$m_t = \frac{P}{16}\left(a^2(\upsilon+1) - r^2(1+3\upsilon)\right) + \frac{m_T}{2}(\upsilon+1)(\ln a - \ln r) - \frac{m_T}{2}\upsilon - D\alpha_T\frac{\Delta T}{h}(1-\upsilon) \tag{28}$$

$$q_r = -\frac{Pr}{2} \tag{29}$$

4. Results and discussion

In this section, some analytical and numerical results are presented for MCD has the geometrical properties of a=0.5 mm and about 0.1 mm thickness h_0 (see section (2.1)). The diaphragm is first pre-stress under radial stress σ_0 then clamped between two plates. The diaphragm is made of one of common material which used in numerous micro electro-mechanical sensors (MEMS) and bioengineering applications; this material is pure aluminum which mechanical and thermal properties are given in Table 1. Table 2 show the mechanical and thermal Loading history applied on the MCD.

4.1 Analytical results

The mechanical behavior of MCD under the previous conditions that have been mentioned we can be discussed in Figs. 4-5. Figs. 4(a)-(f) shows the relation between transverse deflection w, bending moments (m_r, m_t), shear force (q_r) and stress (S_r, S_t) respectively with the MCD radius (r) under varying pressure (P). As shown in the Fig. 4(a) the transverse deflection w is decreased with diaphragm radius (r) and increased with pressure (P) and the maximum deflection occurs at the center of the diaphragm at r=0. Figs. 4(b)-(c) show the bending moment diagram of radial and tangential moment where increased with pressure (P) and the residual moment due to pre-stress is appear in the Fig. 4(b) and the maximum bending moment (m_r, m_t) are occurs at (r=a, r=0) respectively. As shown in Fig. 4(d) the shear force (q_r) is increased with both diaphragm radius and pressure, and the maximum shear force occurs at the at the edge of the diaphragm at r=a. Figs. 4(e)-(f) show the stress at radial and tangential direction of diaphragm where increased with pressure (P) and the pre-stress is appear in Fig. 4(e).

Fig. 5 shows the relation between the radial stress S_r and radial strain e_r, where the radial strain e_r is increased with radial stress S_r. This relation is very important in engineering analysis where

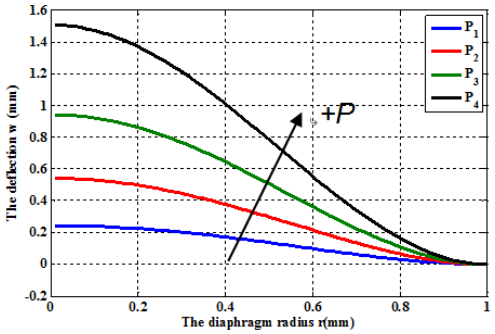

(a) The MCD radius (r) vs. transverse deflection w

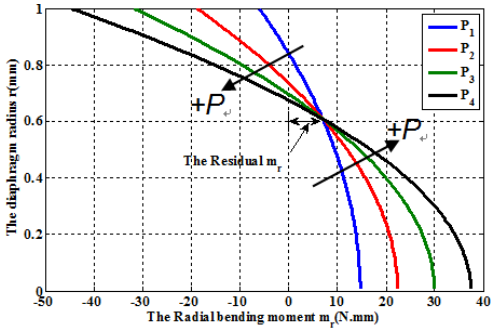

(b) The MCD radius (r) vs. radial bending moment m_r

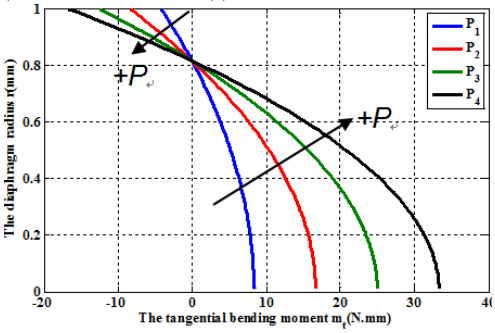

(c) The MCD radius (r) vs. tangential bending moment m_t

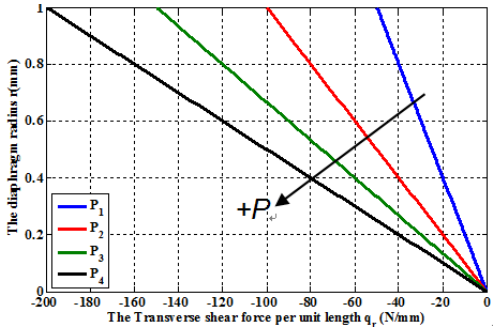

(d) The MCD radius (r) vs. shear force q_r

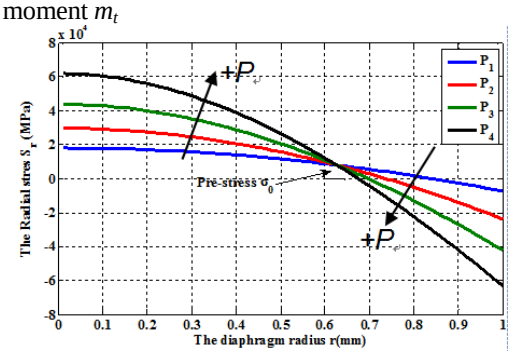

(e) The MCD radius (r) vs. radial stress S_r

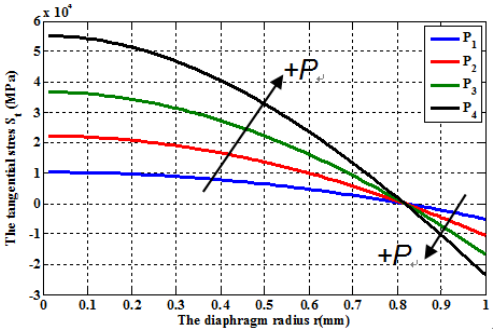

(f) The MCD radius (r) vs. tangential stress S_t

Fig. 4 The mechanical behaviors of the thin MCD under varying pressure P

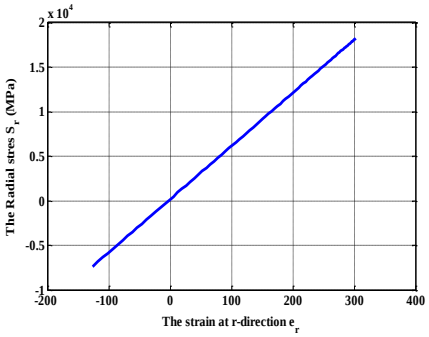

Fig. 5 The relation between the radial stress S_r and radial strain e_r

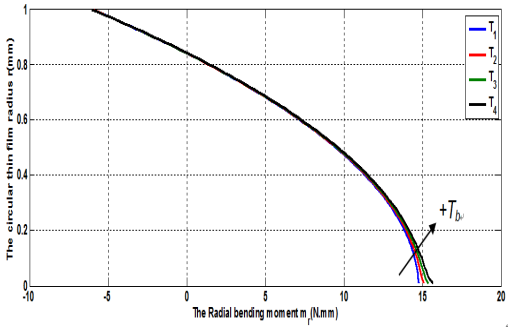

(a) The MCD radius (r) vs. radial bending moment m_r

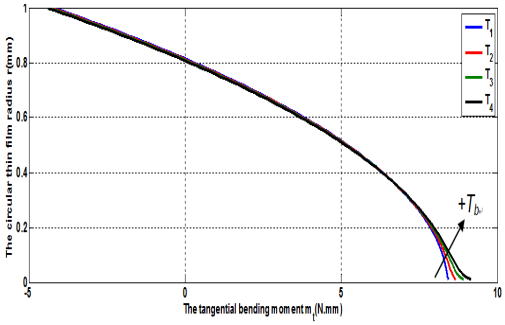

(b) The MCD radius (r) vs. tangential bending moment m_t

Fig. 6 The thermal behaviors of the thin MCD under under varying temperature T_b

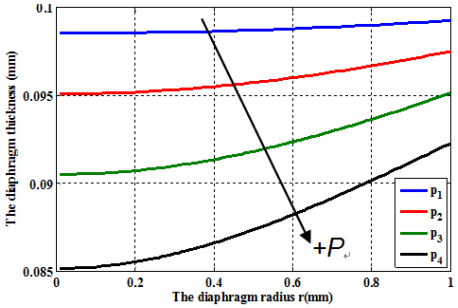

(a) Dome thickness h of the MCD vs. MCD radius r under varying pressure P

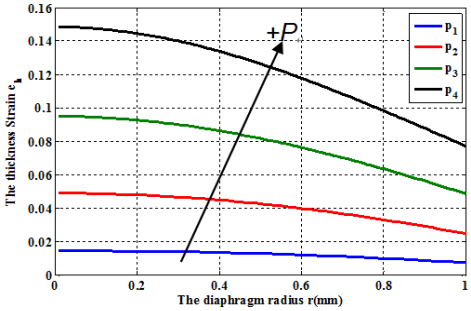

(b) the thickness strain e_h of the MCD vs. MCD radius r under varying pressure P

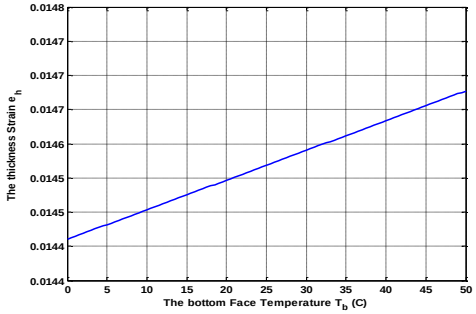

(c) The MCD thickness strain e_h vs. bottom face temperature T_b

Fig. 7 The Thermo-mechanical behavior of MCD thickness deformation under varying pressure P

the Young's modulus E of the diaphragm material from the slop of this liner relation.

The thermal behavior of MCD under the previous conditions that have been mentioned we can be discussed in Fig. 6. Figs. 6(a)-(b) show the relation between bending moments (m_r, m_t) respectively with the MCD radius (r) under varying temperature (T_b), where the maximum bending moments are increased with temperature (T_b).

Fig. 7 shows the MCD thickness deformation behavior across the diaphragm radius (r) under varying pressure (P) and temperature (T_b). As shown in the Fig. 7(a) the dome thickness (h) is increased with diaphragm radius r and decreased with pressure (P), the thickness strain e_h in the

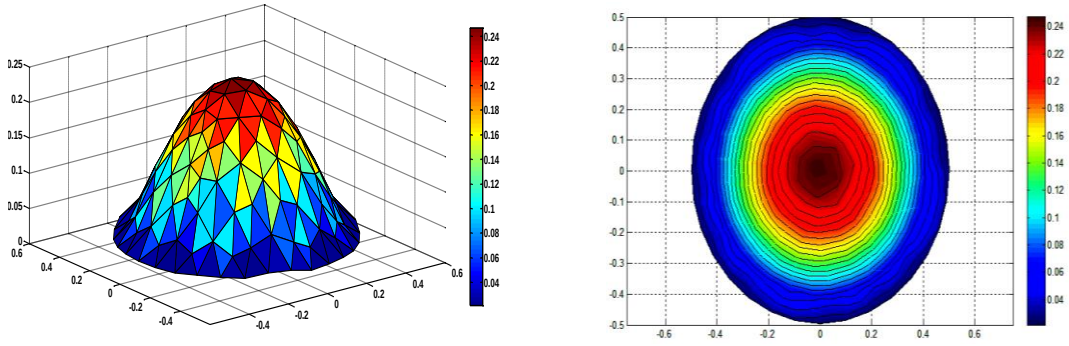

(a) 3D Mesh mode (b) Contour mode

Fig. 8 The finite element simulation for the developed bulge test of MCD

Figs. 7(b)-(c) is increased with the pressure (P) and temperature (T_b) respectively.

4.2 Numerical results

A 3D finite element simulation was selected for modeling the bulge test of MCD by solving Eq. (1), bulge test deflection of MCD w can be obtained. When using FEM to solve problem, the continuous field should be converted to a discrete form, namely, the solution domain should be divided into finite elements. According to finite element analysis, we will carry out imaging of regional triangulation, it is necessary to divided pixel pipe into triangular finite element, because many circular diafragm are round under the circumstances of a smaller number of pixels, we can achieve higher accuracy to use the triangle mesh than rectangular grids, To improve the accuracy of mesh, we will take subdivision method two times imaging region is divided into 982 Elements, the map is as follows in Fig. 8(a).

For the convenience of numerical simulation, the commercially available finite element software using MATLAB is used to build the 3D geometry model of bulge test of MCD and divide the area domain into triangle elements, see Fig. 8(a). The partition results such as node coordinates, boundary condition and relation between elements and nodes are extracted to calculate the deflection of MCD in MATLAB.

The finite element simulation for the developed bulge test of MCD under the previous conditions that have been mentioned we can be discussed in Fig. 8. The MCD is made from pure aluminum which mechanical and thermal properties are given in Table 1. Fig. 8 shows the deformation history of MCD in both 3D Mesh mode and contour mode of clamped MCD at one of applied pressure that we are presented in Table 2. This pressure is $P=P_1=100$ MPa. As shown in the Fig. 8 the maximum deflection occurs at the center of the plate at $r=0$, the maximum deflection w_{max} is found 0.24 mm. The maximum deflection comparison between a finite element model results and analytical calculus are very convergence and closed.

5. Conclusions

In this paper, both analytical and numerical analysis of developed bulge test technique for MCD subjected to thermal and mechanical load has been presented. In the analytical analysis we

have derived the partial differential equation of the MCD. The mechanical and thermal properties relations of the material flow is plotted and discussed. The thickness distribution across the diaphragm radius is discussed to describe the mechanical behavior of the MCD under deformation. The finite element simulation for the developed bulge test of MCD has been shown for the same conditions of the analytical calculus and the comparison between them has been to accuracy and validity of proposed technique. It was found from the results of the comparison the convergence is occurred between the finite element model and analytical model.

References

Ahmed, M. and Hashmi, M.S.J. (1998), "Finite-element analysis of bulge forming applying pressure and in-plane compressive load", *Mater. Process. Technol.*, **77**(1), 95-102.

Brandon, J.F., Lecoanet, H. and Oytana, C. (1979), "A new formulation for the bulging of viscous sheet metals", *J. Mech. Sci.*, **21**(7), 379-386.

Chater, E. and Neale, K.W. (1983), "Finite plastic deformation of a circular membrane under hydrostatic pressure-I", *Mech. Sci.*, **25**(4), 219-233.

Grolleau, V., Gary, G. and Mohr, D. (2008), "Biaxial testing of sheet materials at high strain rates using viscoelastic bars", *Exp. Mech.*, **48**(3), 293-306.

Hill, R. (1950), "A theory of plastic bulging of a metal diaphragm by lateral pressure", *Dub. Philos. Mag. J. Sci.*, **41**(322), 1133-1142.

Hill, R. (1990), "Constitutive modeling of orthotropic plasticity IN sheet metals", *Mech. Phys. Sol.*, **38**(3), 405-417.

Huang, A., Lu, C., Wu, S., Chen, T., Vinci, R.P., Brown, W.L. and Lin, M. (2016), "Viscoelastic mechanical properties measurement of thin Al and Al-Mg films using bulge testing", *Thin Sol. Films*, **618**, 2-7.

Ilahi, M.F. and Paul, T.K. (1985), "Hydrostatic bulging of a circular soft brass diaphragm", *J. Mech. Sci.*, **27**(5), 275-280.

Ilahi, M.F. (1981), "Hydrostatic bulging of a circular aluminum diaphragm", *Mech. Sci.*, **23**(4), 221-227.

Itozaki, H. (1982), "Mechanical properties of composition modulated copper-palladium foils", Ph.D. Dissertation, Northwestern University, U.S.A.

Jung, B., Lee, H., Hwang, K. and Park, H. (2012), "Measurement of mechanical properties of thin films using a combination of the bulge test and nanoindentation", *Trans. Kor. Soc. Mech. Eng. B*, **36**(2), 117-123.

Jung, B., Lee, H., Hwang, K. and Park, H. (2013), "Observation of size effect and measurement of mechanical properties of Ti thin film by bulge test", *Trans. Kor. Soc. Mech. Eng. B*, **37**(1), 19-25.

Kular, G.S. and The, J.H.L. (1972), "The bulging of anisotropic aluminum sheets-a comparison of theory and experiments", *J. Mach. Tool Des. Res.*, **12**(4), 281-296.

Mellor, P.B. (1956), "Stretch forming under fluid pressure", *Mech. Phys. Sol.*, **5**(1), 41-56.

Small, M.K. and Nix, W.D. (1992), "Analysis of the accuracy of the bulge test in determining the mechanical properties of thin-films", *Mater. Res.*, **7**(6), 1553-1563.

Storakers, B. (1966), "Finite plastic deformation of a circular membrane under hydrostatic pressure", *Mech. Sci.*, **8**(10), 619-628.

Suttner, S. and Merklein, M. (2016), "Experimental and numerical investigation of a strain rate controlled hydraulic bulge test of sheet metal", *Mater. Process. Technol.*, **235**, 121-133.

Tang, S.C. (1982), "Large strain analysis of an inflating membrane", *Comput. Struct.*, **15**(1), 71-78.

Ventsel, E. and Krauthammer, T. (2001), *Thin Plates and Shells: Theory: Analysis, and Applications*, Marcel Dekker Inc., New York, U.S.A.

Vlassak, J.J. (1994), "New experimental techniques and analysis methods for the study of mechanical properties of materials in small volumes", Ph.D. Dissertation, Stanford University, California, U.S.A.

Wan, K., Guo, S. and Dillard, D.A. (2003), "A theoretical and numerical study of a thin clamped circular film under an external load in the presence of a tensile residual stress", *Thin Sol. Films*, **425**(1), 150-162.

Wang, N.M. and Shammamy, M.R. (1969), "On the plastic bulging of a circular diaphragm by hydrostatic pressure", *J. Mech. Phys. Sol.*, **17**(1), 43-61.

Xiang, Y., Chen, X. and Vlassak, J.J. (2005), "Plane-strain bulge test for thin films", *Mater. Res. Soc.*, **20**(9), 2360-2370.

Yang, L., Long, S., Ma, Z. and Wang, Z. (2014), "Accuracy analysis of plane-strain bulge test for determining mechanical properties of thin films", *Trans. Nonfer. Metals Soc. China*, **24**(10), 3265-3273.

Zeghloul, A. (1991), "Influence of material parameters on the hydrostatic bulging of a circular diaphragm", *Mech. Sci.*, **33**(3), 229-243.

Zhang, J., Sun, Y., Li, D., Cao, Y., Wang, Z., Ma, J. and Zhao, G. (2015), "Modeling the mechanics of graphene-based polymer composite film measured by the bulge test", *Phys. D: Appl. Phys.*, **48**(42), 425302.

NS